Progress In Electromagnetics Research C, Vol. 84, 23–33, 2018

The Direction-of-Arrival and Polarization Estimation Using Coprime Array: A Reconstructed Covariance Matrix Approach

Wen Dong*, Ming Diao, and Lipeng Gao

Abstract—In this paper, we propose a novel direction of arrival (DOA) and polarization estimation method to address the problem of a coprime polarization-sensitive array (PSA). For a PSA, there may be a zero element in the covariance matrix when the polarized signal comes from a specific direction. To overcome this problem, we utilize the reconstructed received data to obtain a new covariance matrix whose elements are all non-zero. Then, the coprime MUSIC and sparse signal reconstruction algorithms are used for DOA estimation. In addition, the power of noise can be estimated in this polarization model, which improves upon the sparse signal reconstruction algorithm. Compared with the normalized algorithm, the proposed method offers favorable performance in terms of accuracy. Furthermore, our method can identify the peaks of the true DOAs at a low signal-to-noise ratio (SNR). The simulation results demonstrate the effectiveness of the proposed method.

1. INTRODUCTION

Direction of arrival (DOA) estimation using a polarization-sensitive array (PSA) has received considerable attention in many practical applications involving radar, navigation, and communication [1, 2]. PSAs, which can receive three directions of the electric field, has many advantages, such as high accuracy, strong resolution, and good anti-jamming capability. Thus, the PSA has played an important role in signal processing in recent decades [3–8]. Many DOA and polarization estimation using dipole triads algorithms have been proposed [9–19]. Polarized multiple signal classification (MUSIC) [20, 21] and the polarized signal parameters via rotational invariance technique (ESPRIT) [22, 23] are two major approaches. However, conventional source estimation algorithms are limited by the degrees of freedom (DOFs). In a uniform linear array, M physical sensors can identify up to $M-1$ sources, and much of the information in the covariance matrix is lost. Many sparse arrays have been proposed to identify more sources with the same number of physical sensors [24–27].

Recently, the coprime array has received substantial attention due to its high DOFs [28–31]. When M and N are coprime, a coprime array can achieve $O(MN)$ DOFs with $(M+N)$ elements. To obtain a contiguous virtual array, we need to calculate the difference coarray to obtain the steering vector of the virtual array. However, this technique employs only a portions of the difference coarray because there are several elements in the virtual array called holes. To overcome this problem, two important approaches have been proposed. In [32], multiple frequencies are utilized to fill in the holes of the coprime array. In [33], a new approach to super-resolution spectrum estimation using a coprime pair of samplers is proposed. These two technologies can exploit all the DOFs for DOA estimation. Then, the received data can be regarded as an equivalent received signal of the virtual array. In this model, the reconstructed received data behave as a single point. However, the rank of the covariance matrix of the reconstructed received data is one. Therefore, the MUSIC algorithm based on spatial smoothing [34] and the sparse reconstruction algorithm [35] are proposed for cases of multiple incident

Received 20 March 2018, Accepted 29 April 2018, Scheduled 11 May 2018
* Corresponding author: Wen Dong (343720065@qq.com).
The authors are with the College of Information and Communication Engineering, Harbin Engineering University, China.

sources. Moreover, the literature [36] introduces a sparse recovery method to detect multiple sources. In [37], DOA estimation is performed via coprime array; however, the performance of these algorithms is poor because they use the PSA directly.

In this paper, we propose a reconstructed covariance matrix method to improve DOA and polarization estimation. In this way, all the elements in the covariance matrix are non-zero, and the performance of the two DOA estimation algorithms is improved. Specifically, the power of noise, which is difficult to estimate, is obtained to improve the sparse reconstruction algorithm using the PSA. Then, this improved method is compared with the conventional coprime algorithm.

The remainder of this paper is organized as follows. In Section 2, we introduce the signal model and coprime array configuration. Section 3 presents the proposed method based on the reconstructed covariance matrix. In Section 4, we compare the performance of the proposed method with that of two normalized methods.

The mathematical notation used throughout this paper is denoted as follows. $(\cdot)^*$, $(\cdot)^T$, $(\cdot)^H$, $E\{\cdot\}$, and $\otimes$ denote the conjugate, transpose, conjugate transpose, statistical expectation, and Kronecker product, respectively. Additionally, $\|\cdot\|$ denotes the modulus of the internal entity. $\|\cdot\|_0$ denotes the l_0 norm, and $\|\cdot\|_1$ and $\|\cdot\|_2$, respectively, denote the l_1 and l_2 norms.

2. SYSTEM MODEL

As illustrated in Figure 1, a coprime array consists of two uniform linear subarrays, which are located in the same line and share the same element in the original point. All elements contain a pair of orthogonal cross dipoles parallel to the x-, y- and z-axes. The first subarray has $2M$ equal-spaced sensors, and the other subarray has N equal-spaced sensors, where M and N are coprime numbers. The unit inter-element d is $\lambda/2$, where λ denotes the signal wavelength. The element spaces of the two subarrays are N units and M units. Here, we assume $M < N$ and double M to overcome the problem of missing holes discussed in [33]. Hence, the $2M + N - 1$ element positions from the original point can be obtained by

$$S = \{Nmd, 0 \leq m \leq 2M - 1\} \cup \{Mnd, 0 \leq n \leq N - 1\}, \tag{1}$$

and the difference coarray can be calculated as

$$S_0 = \{\pm(Nmd - Mnd)\}. \tag{2}$$

Because M and N are coprime, contiguous elements can be obtained from $-(MN + M - 1)d$ to $(MN + M - 1)d$.

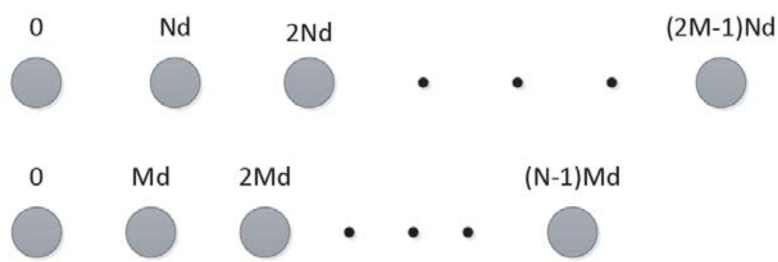

Figure 1. The system model of two subarrays.

Consider K uncorrelated narrowband signals impinging upon a PSA with elevation angles θ_k, where $k = 1, \ldots, K$. Since each sensor can receive three electric field components, as shown in [4], the data vector received at time t is expressed as

$$\mathbf{x}(t) = \begin{bmatrix} \mathbf{x}_1(t) \\ \mathbf{x}_2(t) \\ \mathbf{x}_3(t) \end{bmatrix} = \begin{bmatrix} \sum_{k=1}^{K} \mathbf{a}(\theta_k) e_{x,k} s_k(t) + \mathbf{n}_1(t) \\ \sum_{k=1}^{K} \mathbf{a}(\theta_k) e_{y,k} s_k(t) + \mathbf{n}_2(t) \\ \sum_{k=1}^{K} \mathbf{a}(\theta_k) e_{z,k} s_k(t) + \mathbf{n}_3(t) \end{bmatrix} = \begin{bmatrix} \mathbf{A}\mathbf{E}_x \mathbf{s}(t) + \mathbf{n}_1(t) \\ \mathbf{A}\mathbf{E}_y \mathbf{s}(t) + \mathbf{n}_2(t) \\ \mathbf{A}\mathbf{E}_z \mathbf{s}(t) + \mathbf{n}_3(t), \end{bmatrix} \tag{3}$$

where

$$\begin{bmatrix} e_{x,k} \\ e_{y,k} \\ e_{z,k} \end{bmatrix} = \underbrace{\begin{bmatrix} 0 & \cos\theta_k \\ 1 & 0 \\ 0 & -\sin\theta_k \end{bmatrix}}_{\boldsymbol{\Xi}(\theta_k)} \underbrace{\begin{bmatrix} \cos\gamma_k \\ \sin\gamma_k e^{j\eta_k} \end{bmatrix}}_{\mathbf{h}_{\gamma_k,\eta_k}} \tag{4}$$

and

$$\mathbf{a}(\theta_k) = \left[1, e^{j\frac{2\pi p_1}{\lambda}\sin(\theta_k)}, \ldots, e^{j\frac{2\pi p_{2M+N-1}}{\lambda}\sin(\theta_k)}\right]^T. \tag{5}$$

In Eq. (3), $s_k(t)$ is the kth source signal vector, and $\mathbf{n}(t)$ is the corresponding noise vector. In Eq. (4), $-\pi/2 \le \theta < \pi/2$ denotes the signal's elevation angle; $0 \le \gamma < \pi/2$ represents the auxiliary polarization angle; $0 \le \eta < 2\pi$ is the polarization phase difference. In Eq. (5), p_i is the positions of the array sensors, where $p_i \in S$, as shown in Figure 2.

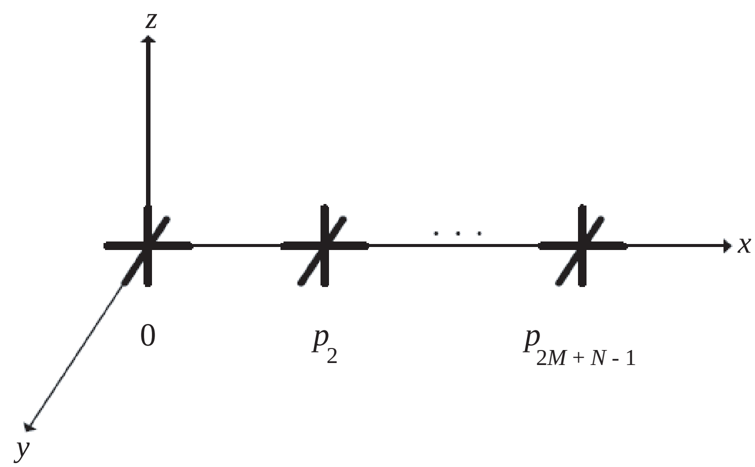

Figure 2. Structure of a triple-polarization coprime array.

The covariance matrix is obtained as

$$\mathbf{R}_{xx} = E[\mathbf{x}(t)\mathbf{x}^H(t)] = \begin{bmatrix} E[\mathbf{x}_1(t)\mathbf{x}_1^H(t)] & E[\mathbf{x}_1(t)\mathbf{x}_2^H(t)] & E[\mathbf{x}_1(t)\mathbf{x}_3^H(t)] \\ E[\mathbf{x}_2(t)\mathbf{x}_1^H(t)] & E[\mathbf{x}_2(t)\mathbf{x}_2^H(t)] & E[\mathbf{x}_2(t)\mathbf{x}_3^H(t)] \\ E[\mathbf{x}_3(t)\mathbf{x}_1^H(t)] & E[\mathbf{x}_3(t)\mathbf{x}_2^H(t)] & E[\mathbf{x}_3(t)\mathbf{x}_3^H(t)] \end{bmatrix}, \tag{6}$$

where $\mathbf{R}_{xx} \in \mathbb{C}^{3(2M+N-1)\times 3(2M+N-1)}$. Note that the entries of the covariance matrix correspond to different lags. Unfortunately, some covariance matrix elements are zero in special cases. For example, $e_{y,k} = e_{z,k} = 0$ when $\gamma = 0°$. To avoid this problem, we reconstruct the covariance matrix as follows

$$\begin{aligned} \mathbf{R}_{xx} &= E\left[\mathbf{x}_1\mathbf{x}_1^H + \mathbf{x}_2\mathbf{x}_2^H + \mathbf{x}_3\mathbf{x}_3^H\right] \\ &= \mathbf{A}E\left\{\mathbf{E}_x\mathbf{s}(t)\mathbf{s}^H(t)\mathbf{E}_x^H\right\}\mathbf{A}^H + \mathbf{A}E\left\{\mathbf{E}_y\mathbf{s}(t)\mathbf{s}^H(t)\mathbf{E}_y^H\right\}\mathbf{A}^H + \mathbf{A}E\left\{\mathbf{E}_z\mathbf{s}(t)\mathbf{s}^H(t)\mathbf{E}_z^H\right\}\mathbf{A}^H \\ &= \mathbf{A}\begin{bmatrix} \left(\|e_{x,1}\|^2 + \|e_{y,1}\|^2 + \|e_{z,1}\|^2\right)\rho_1^2 & & \\ & \ddots & \\ & & \left(\|e_{x,K}\|^2 + \|e_{y,K}\|^2 + \|e_{z,K}\|^2\right)\rho_K^2 \end{bmatrix}\mathbf{A}^H \\ &\quad + \left(\sigma_1^2 + \sigma_2^2 + \sigma_3^2\right)\mathbf{I}, \end{aligned} \tag{7}$$

where ρ_k^2 is the power of the kth source, σ^2 the noise power, and $\mathbf{I} \in \mathbb{C}^{(2M+N-1)\times(2M+N-1)}$ the unit matrix. Now, $\mathbf{R}'_{xx} \in \mathbb{C}^{(2M+N-1)}$, and all the elements in the reconstructed covariance matrix are non-zero. According to Eq. (4), $\|e_{x,k}\|^2 + \|e_{y,k}\|^2 + \|e_{z,k}\|^2 = 1$. Then, the covariance matrix becomes

$$\mathbf{R}'_{xx} = \mathbf{A}\begin{bmatrix} \rho_1^2 & & \\ & \ddots & \\ & & \rho_K^2 \end{bmatrix}\mathbf{A}^H + \tilde{\sigma}^2\mathbf{I}. \tag{8}$$

We make the following basic assumptions:

(1). All the sources are completely polarized waves that are uncorrelated with each other.

(2). $\mathbf{n}(t)$ is a Gaussian random processes that is uncorrelated with $s(t)$. The power of noise is constant, which means $\sigma_1^2 = \sigma_2^2 = \sigma_3^2 = \sigma^2$ and $\tilde{\sigma}^2 = 3\sigma^2$.

(3). The array is calibrated, and the mutual coupling among the antenna array elements is neglected.

3. COPRIME ALGORITHM

In this section, we use the MUSIC and sparse reconstruction algorithms based on the reconstructed covariance matrix to estimate the DOA. To obtain the contiguous steering vector, we vectorize $\mathbf{R}'_{xx}$, which yields

$$\mathbf{z} = \mathrm{vec}(\mathbf{R}'_{xx}) = \tilde{\mathbf{A}}\mathbf{b} + \tilde{\sigma}^2\mathbf{i}, \tag{9}$$

where $\tilde{\mathbf{A}} = [\mathbf{a}^*(\theta_1) \otimes \mathbf{a}(\theta_1), \dots, \mathbf{a}^*(\theta_K) \otimes \mathbf{a}(\theta_K)] \in \mathbb{C}^{(2M+N-1)^2 \times K}$, $\mathbf{b} = [\rho_1^2, \dots, \rho_K^2]^T$, and $\mathbf{i} = \mathrm{vec}(\mathbf{I}) \in \mathbb{C}^{(2M+N-1)^2}$. The vector $\mathbf{z}$ is the received signal vector from a virtual array with corresponding steering matrix $\tilde{\mathbf{A}}'$. However, many repeated rows in matrix $\tilde{\mathbf{A}}$ must be removed, and the remaining rows should be sorted. The constructed $\tilde{\mathbf{A}}' \in \mathbb{C}^{(2MN+2M-1) \times K}$ acts as a consecutive ULA with $(2MN + 2M - 1)$ sensors located from $-(MN + M - 1)$ to $(MN + M - 1)$. The constructed vector $\mathbf{z}'$ can be expressed as

$$\mathbf{z}' = \tilde{\mathbf{A}}'\mathbf{b} + \tilde{\sigma}^2\mathbf{i}', \tag{10}$$

where the $(MN + M)$th element of vector $\mathbf{i}'$ is one and the other elements are zero.

3.1. MUSIC Approach

Note that $\mathbf{z}'$ represents a single snapshot, and the rank of the covariance matrix is one. Spatial smoothing technique is used to overcome the problem of multiple incident sources. With Equation (10), the consecutive virtual ULA can be divided into $(MN+M)$ overlapping subarrays with $(MN+M)$ sensors for each subarray, and the initial points of these subarrays are located from $-(MN + M - 1)$ to 0. Then, the data received data by the ith subarray can be written as

$$\mathbf{z}'_i = \mathbf{z}'(i : MN + M - 1 + i, 1), \tag{11}$$

where $i = 1, 2, \dots, (MN + M)$. The covariance matrix of the ith subarray can be calculated as follows

$$\mathbf{R}'_i = \mathbf{z}'_i \mathbf{z}'^H_i. \tag{12}$$

To obtain the full rank covariance matrix, we reconstruct the data with spatial smoothing as

$$\mathbf{R}_s = \frac{1}{MN + M} \sum_{i=1}^{MN+M} \mathbf{R}'_i. \tag{13}$$

The size of the spatially smoothed covariance matrix is $(MN+M) \times (MN+M)$, which has a rank of $(MN + M)$. Hence, $MN + M$ sources can be estimated by using only $2M + N - 1$ physical sensors, and the DOAs can be obtained by using the conventional MUSIC algorithm [21]. Assume that L is the number of snapshots; the main steps of the proposed method are summarized in Algorithm 1.

Algorithm 1 Steps in the Proposed Method.

Input: $\mathbf{x}(1), \mathbf{x}(2), \cdots, \mathbf{x}(L)$
1. Obtain $\mathbf{x}$ according to Equation (3)
DOA Estimation:
2. Reconstruct the covariance matrix via Equation (7)
3. Vectorize $\mathbf{R}'_{xx}$ according to Equation (9)
4. Obtain $\mathbf{z}'$ according to Equation (10)
5. Calculate the covariance matrix of the ith virtual subarray using Equation (12)
6. Average all the covariance matrices of the subarrays from Equation (13)
7. Estimate the DOAs through $\mathbf{R}_s$ using the MUSIC algorithm

3.2. Sparse Reconstruction Approach

In this subsection, we solve Eq. (10) in terms of the sparse signal recovery through compressive sensing. The sparse representation can be written as

$$\mathbf{z}' = \mathbf{A}_s \mathbf{b}_s + \tilde{\sigma}^2 \mathbf{i}', \tag{14}$$

where $\mathbf{A}_s = [\mathbf{b}(\tilde{\theta}_1), \mathbf{b}(\tilde{\theta}_2), \ldots, \mathbf{b}(\tilde{\theta}_Q)] \in \mathbb{C}^{(2MN+2M-1)\times Q}$ is an over-complete basis ($Q \gg K$), and $\mathbf{b}_s = [\bar{\rho}_1^2, \bar{\rho}_2^2, \ldots, \bar{\rho}_Q^2]^T$ is K-sparse, which can be expressed as

$$\bar{\rho}_i = \begin{cases} \rho_k, & \tilde{\theta}_i \in [\theta_1, \theta_2, \ldots, \theta_K] \\ 0, & \tilde{\theta}_i \notin [\theta_1, \theta_2, \ldots, \theta_K] \end{cases}, \quad i = 1, 2, \ldots, Q. \tag{15}$$

Then, the optimal solution of Equation (14) can be represented as the following constrained minimization problem

$$\begin{aligned} \hat{\mathbf{b}}_s &= \arg\min_{\mathbf{b}_s} \|\mathbf{b}_s\|_0 \\ \text{s.t.} \quad \mathbf{z}' &= \mathbf{A}_s \mathbf{b}_s + \tilde{\sigma}^2 \mathbf{i}' \end{aligned} \tag{16}$$

.

Unfortunately, the minimization problem of the l_0-norm is NP hard. By using the l_1-norm to replace the l_0-norm, Equation (16) can be reformulated as

$$\begin{aligned} \widehat{\mathbf{b}}_s &= \arg\min_{\mathbf{b}_s} \|\mathbf{b}_s\|_1 \\ \text{s.t.} \quad \mathbf{z}' &= \mathbf{A}_s \mathbf{b}_s + \tilde{\sigma}^2 \mathbf{i}'. \end{aligned} \tag{17}$$

Equation (17) is then convex, and the above optimization problem can be defined as

$$\widehat{\mathbf{b}}_s = \arg\min_{\mathbf{b}_s} \left[\frac{1}{2} \left\| \mathbf{z}' - \mathbf{A}_s \mathbf{b}_s - \tilde{\sigma}^2 \mathbf{i}' \right\|_2 + c \|\mathbf{b}_s\|_1 \right], \tag{18}$$

where c is a penalty parameter that balances the tradeoff between the error of the reconstructed covariance matrix and the sparsity of the spatial spectrum. Note that we add the noise vector $\tilde{\sigma}^2 \mathbf{i}'$, which is hard to estimate in other models because the number of sources is greater than the number of physical sensors. However, we can obtain a covariance matrix of size $3(2M+N-1) \times 3(2M+N-1)$ from Equation (6). Then, we can obtain $3(2M+N-1)-K$ smaller eigenvalues through the eigen-decomposition of $\mathbf{R}_{xx}$.

$$\mathbf{R}_{xx} = \mathbf{U} \Lambda \mathbf{U}^H, \tag{19}$$

where $\Lambda = \mathrm{diag}\{\kappa_1, \ldots, \kappa_{3(2M+N-1)-K}, \ldots, \kappa_{3(2M+N-1)}\}$. The power of noise $\hat{\sigma}^2$ can be obtained by averaging these smaller eigenvalues; then, $\tilde{\sigma}^2 = 3\hat{\sigma}^2$.

$$\hat{\sigma}^2 = \frac{1}{3(2M+N-1)-K} \sum_{i=1}^{3(2M+N-1)-K} \kappa_i \tag{20}$$

The DOA estimation $\hat{\theta} = \{\hat{\theta}_1, \hat{\theta}_2, \dots, \hat{\theta}_K\}$ can be obtained according to the positions of non-zeros in $\widehat{\mathbf{b}}_s$; the main steps of the proposed method are summarized in Algorithm 2.

Algorithm 2 Steps in the Proposed Method.

Input: $\mathbf{x}(1), \mathbf{x}(2), \cdots, \mathbf{x}(L)$
1. Obtain $\mathbf{x}$ according to Equation (3)

DOA Estimation:
2. Reconstruct the covariance matrix via Equation (7)
3. Vectorize $\mathbf{R}'_{xx}$ according to Equation (9)
4. Obtain $\mathbf{z}'$ according to Equation (10)
5. Obtain the dictionary matrix $\mathbf{A}_s$
6. Calculate the noise power via Equations (19) and (20).
7. Compute $\widehat{\mathbf{b}}_s$ via Equation (18)
8. Estimate the DOAs according to the positions of non-zeros in $\widehat{\mathbf{b}}_s$

3.3. Polarization Parameter Estimation

In this section, we estimate the polarization parameters using the generalized eigenvalue method [38]. From the MUSIC algorithm, we can know

$$\mathbf{h}_{\gamma,\eta}^H \mathbf{D}_\theta^H \tilde{\mathbf{U}}_N \tilde{\mathbf{U}}_N^H \mathbf{D}_\theta \mathbf{h}_{\gamma,\eta} = 0 \tag{21}$$

where $\mathbf{D}_{\hat{\theta}} = \mathbf{A}(\hat{\theta}) \otimes \mathbf{\Xi}(\hat{\theta})$ which can be obtained from Equations (3) and (4) based on the estimate $\hat{\theta}$. $\mathbf{H}(\hat{\theta}) = \mathbf{D}_{\hat{\theta}}^H \mathbf{U}_\mathbf{N}^H \mathbf{U}_N \mathbf{D}_{\hat{\theta}}$, and $\mathbf{U}_N = \mathbf{U}(:, 1 : 3(2M+N-1)-K)$ is the noise subspace. Then Equation (21) can be written as follow

$$\begin{aligned}\{\hat{\gamma}, \hat{\eta}\} &= \arg\min_{\gamma,\eta} \left\{ \left(\frac{\mathbf{D}_{\hat{\theta}} \mathbf{h}_{\gamma,\eta}}{\left\| \mathbf{D}_{\hat{\theta}} \mathbf{h}_{\gamma,\eta} \right\|} \right)^H \tilde{\mathbf{U}}_N \tilde{\mathbf{U}}_N^H \left(\frac{\mathbf{D}_{\hat{\theta}} \mathbf{h}_{\gamma,\eta}}{\left\| \mathbf{D}_{\hat{\theta}} \mathbf{h}_{\gamma,\eta} \right\|} \right) \right\} = \arg\min_{\gamma,\eta} \left\{ \frac{\mathbf{h}_{\gamma,\eta}^H \mathbf{H}(\hat{\theta}) \mathbf{h}_{\gamma,\eta}}{\mathbf{h}_{\gamma,\eta}^H \mathbf{D}_{\hat{\theta}}^H \mathbf{D}_{\hat{\theta}} \mathbf{h}_{\gamma,\eta}} \right\} \\ &= \arg\min_{\mathbf{h}_{\gamma,\eta} \neq 0} \left\{ \frac{\mathbf{h}_{\gamma,\eta}^H \mathbf{H}(\hat{\theta}) \mathbf{h}_{\gamma,\eta}}{\mathbf{h}_{\gamma,\eta}^H \mathbf{D}_{\hat{\theta}}^H \mathbf{D}_{\hat{\theta}} \mathbf{h}_{\gamma,\eta}} \right\} = \arg\min_{\mathbf{h}_{\gamma,\eta}^H \mathbf{D}_{\hat{\theta}}^H \mathbf{D}_{\hat{\theta}} \mathbf{h}_{\gamma,\eta} = 1} \left\{ \frac{\mathbf{h}_{\gamma,\eta}^H \mathbf{H}(\hat{\theta}) \mathbf{h}_{\gamma,\eta}}{\mathbf{h}_{\gamma,\eta}^H \mathbf{D}_{\hat{\theta}}^H \mathbf{D}_{\hat{\theta}} \mathbf{h}_{\gamma,\eta}} \right\}\end{aligned} \tag{22}$$

Now the the minimization problem turn into a optimization problem.

$$\begin{aligned}&\min_{\mathbf{h}_{\gamma,\eta}} \mathbf{h}_{\gamma,\eta}^H \mathbf{H}(\theta_k) \mathbf{h}_{\gamma,\eta} \\ &\text{s.t.} \quad \mathbf{h}_{\gamma,\eta}^H \mathbf{D}_\theta^H \mathbf{D}_\theta \mathbf{h}_{\gamma,\eta} = 1\end{aligned} \tag{23}$$

Then the polarization angle γ and the polarization phase difference η can be estimated as

$$\begin{aligned}c\hat{\mathbf{h}}_{\gamma,\eta} &= \hbar_{\min} \left\{ \mathbf{H}(\hat{\theta}), \mathbf{D}_{\hat{\theta}}^H \mathbf{D}_{\hat{\theta}} \right\} \\ \hat{\gamma} &= \arctan \left\{ \left| \hat{\mathbf{h}}_{\gamma,\eta}(2) / \hat{\mathbf{h}}_{\gamma,\eta}(1) \right| \right\} \\ \hat{\eta} &= \arg \left\{ \hat{\mathbf{h}}_{\gamma,\eta}(2) / \hat{\mathbf{h}}_{\gamma,\eta}(1) \right\}\end{aligned} \tag{24}$$

where c is a non-zero value.

4. SIMULATION

In this section, several simulations are presented to illustrate the feasibility of the proposed method based on a coprime array consisting of a pair of sparse ULAs, as shown in Figure 2. We set $2M = 2\times3 = 6$ and $N = 5$. Hence, $2M + N - 1 = 10$ physical sensors are located at $[0, 3, 5, 6, 9, 10, 12, 15, 20, 25]d$. Assume that there are $K = 14$ far-field narrowband completely polarized electromagnetic wave sources impinging upon the array. These source signals are uniformly distributed from $-52°$ to $52°$, auxiliary polarization $28°$ to $80°$, and polarization phase difference $40°$ to $170°$. In the MUSIC and sparse reconstruction algorithms, the spatial grid is uniform with a $0.1°$ sampling interval within $[-60°, 60°]$. The penalty parameter $c = 0.25$ is chosen for the optimization problem in Eq. (18). Two hundred independent Monte Carlo runs are conducted for the following simulations. The root-mean-square error (RMSE) is chosen as the performance metric with different SNRs and is defined as

$$\text{RMSE} = \sqrt{\frac{1}{200K}\sum_{i=1}^{200}\sum_{k=1}^{K}(\hat{\theta}_k - \theta_k)^2} \tag{25}$$

$$\text{SNR} = 10\log_{10}\frac{\rho^2}{\sigma^2}. \tag{26}$$

In the first simulation, we plot the normalized spectrum of the proposed method based on the reconstructed covariance matrix and the conventional coprime algorithm. The simulation parameters

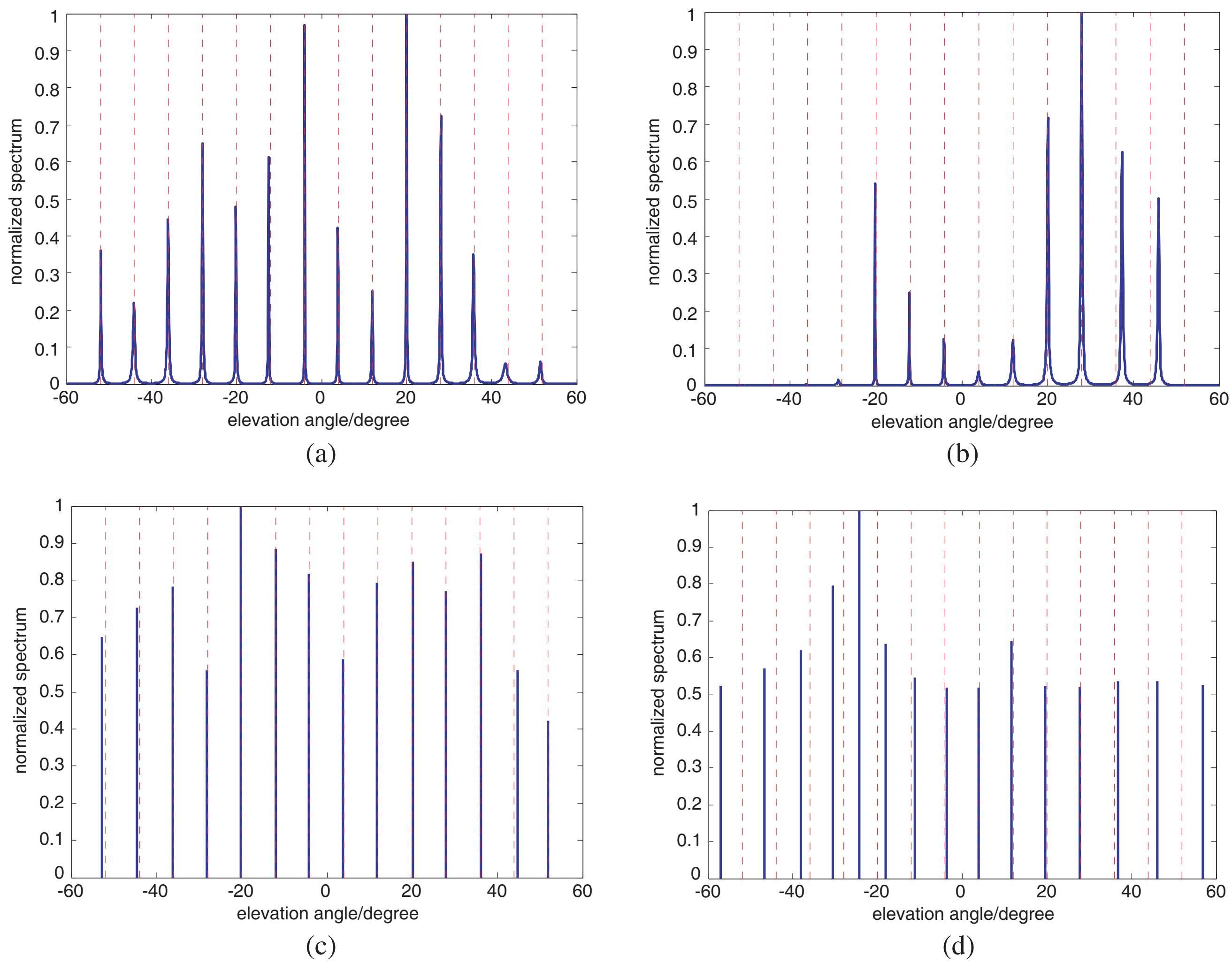

Figure 3. Spatial spectrum comparison with a fixed SNR of -5 dB and 1000 snapshots. (a) Proposed MUSIC algorithm based on the matrix reconstruction. (b) Coprime MUSIC algorithm in [33]. (c) Proposed sparse signal algorithm based on the matrix reconstruction. (d) Sparse signal algorithm in [39].

are set to SNR $= -5$ dB and number of snapshots $L = 1000$. The proposed method can plot all the peaks of the 14 sources, as shown in Figure 3(a), and the peaks are deficient, as shown in Figure 3(b). By contrast, Figure 3(d) shows a spurious peak, whereas no spurious peak is present in Figure 3(c). Hence, the proposed method correctly identifies the true source spectra when the input SNR is low.

In the second simulation, the RMSE of the proposed method versus the SNR is investigated. The results from Figures 4–6 demonstrate that the proposed method yields more accurate results than those of the conventional method because there are no irregular spurious peaks around the signal response peaks for the spatial spectrum when using the reconstructed covariance matrix. By contrast, the conventional coprime MUSIC algorithm and sparse signal reconstruction algorithm have irregular spurious peaks or missing spectrum peaks when some of the covariance matrix elements are zero, as discussed in Section 2.

In the third simulation, the RMSEs of the proposed method and the normalized method are compared and displayed in Figure 7. We set SNR $= 0$ dB. The proposed methods clearly outperform the normalized method, and the coprime MUSIC approach outperforms the sparse reconstruction method for all numbers of snapshots.

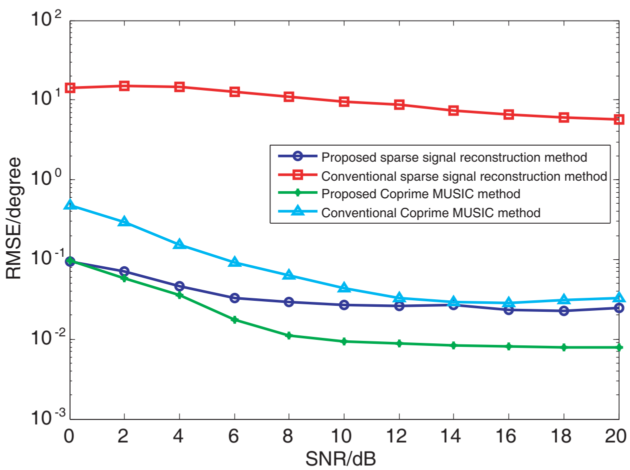

Figure 4. RMSE of θ estimates versus SNR for two method with fixed snapshot number 1000.

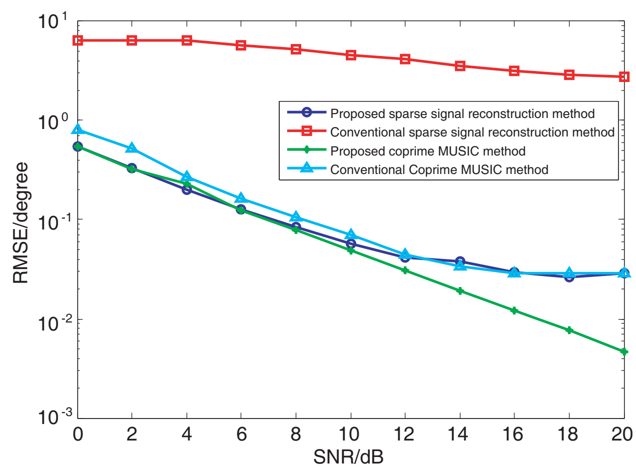

Figure 5. RMSE of γ estimates versus SNR with snapshot number 1000.

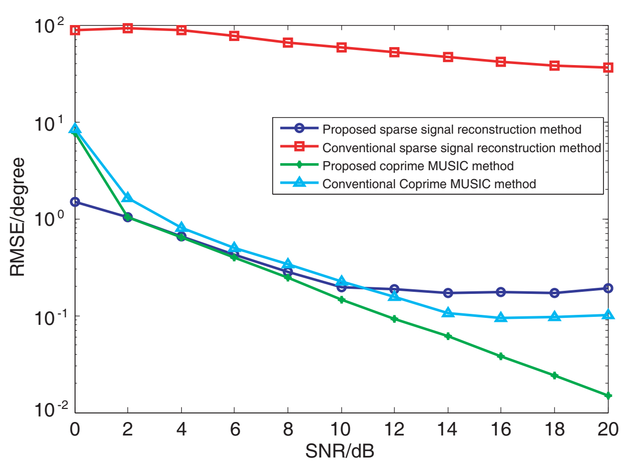

Figure 6. RMSE of η estimates versus SNR with snapshot number 1000.

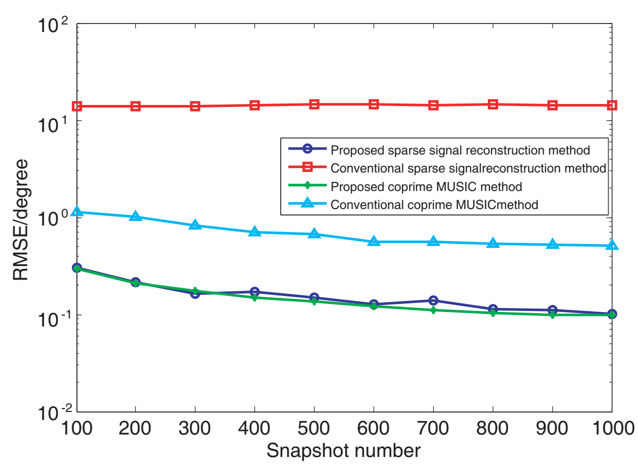

Figure 7. RMSE of the θ estimates versus number of snapshots for two methods with a fixed SNR $= 0$.

5. CONCLUSIONS

In this paper, a reconstructed covariance matrix method is proposed for a coprime PSA. The proposed method first reconstructs the received data and then obtains a covariance matrix that has no zero elements. Then, we can use the coprime MUSIC and sparse signal reconstruction algorithm for the DOA estimation. Finally, we can estimate the polarization parameters by using generalized eigenvalue methods. Hence, the coprime PSA can increase the number of DOFs to $O(MN+M)$ with $2M+N-1$ sensors while maintaining high accuracy. The simulation results show that the proposed method improves upon the traditional algorithms.

ACKNOWLEDGMENT

This work was supported in part by the National Natural Science Foundation of China under Grant 61571149. The authors would like to thank the anonymous reviewers and the associate editor for their valuable comments and suggestions, which have greatly improved the quality of this paper.

REFERENCES

1. Yuan, X., "Estimating the DOA and the polarization of a polynomial-phase signal using a single polarized vector-sensor," *IEEE Transactions on Signal Processing*, Vol. 60, 1270–1282, 2012.
2. Si, W., P. Zhao, and Z. Qu, "Two-dimensional DOA and polarization estimation for a mixture of uncorrelated and coherent sources with sparsely-distributed vector sensor array," *Sensors*, Vol. 16, 1–23, 2016.
3. Goossens, R. and H. Rogier, "A hybrid UCA-RARE/root-MUSIC approach for 2-D direction of arrival estimation in uniform circular arrays in the presence of mutual coupling," *IEEE Transactions on Antennas and Propagation*, Vol. 55, 841–849, 2007.
4. Wong, K. T., L. Li, and M. D. Zoltowski, "Root-MUSIC-based direction-finding and polarization-estimation using diversely-polarized possibly-collocated antennas," *IEEE Antennas Wirel. Propag. Lett.*, Vol. 3, 129–132, 2004.
5. Rahamim, D., J. Tabrikian, and R. Shavit, "Source localization using vector sensor array in a multipath environment," *IEEE Transactions on Signal Processing*, Vol. 52, 3096–3103, 2004.
6. He, J., S. Jiang, and J. Wang, "Polarization difference smoothing for direction finding of coherent signals," *IEEE Transactions on Aerospace and Electronic Systems*, Vol. 46, 469–480, 2010.
7. Xu, Y. and Z. Liu, "Polarimetric angular smoothing algorithm for an electromagnetic vector-sensor array," *IET Radar Sonar Navig.*, Vol. 1, 230–240, 2007.
8. Diao, M. and C. L. An, "Direction finding of coexisted independent and coherent signals using electromagnetic vector sensor," *J. Syst. Eng. Electron.*, Vol. 23, 481–487, 2012.
9. Yuan, X., K. T. Wong, Z. Xu, and K. Agrawal, "Various triad compositions of collocated dipoles/loops, for direction finding and polarization estimation," *IEEE Sensors Journal*, Vol. 12, 1763–1771, 2012.
10. Wong, K. T. and X. Yuan, "Vector cross-product direction-finding with an electromagnetic vector-sensor of six orthogonally oriented but spatially non-collocating dipoles/loops," *IEEE Transactions on Signal Processing*, Vol. 59, 160–171, 2010.
11. Song, Y., X. Yuan, and K. T. Wong, "Corrections to vector cross-product direction-finding with an electromagnetic vector-sensor of six orthogonally oriented but spatially non-collocating dipoles/loops," *IEEE Transactions on Signal Processing*, Vol. 62, 1028–1030, 2014.
12. Song, Y., K. T. Wong, and F. Chen, "'Blind' calibration of vector sensors whose dipole/loop triads deviate from their nominal gains/phases/orientations/locations," *Radio Science*, Vol. 52, 1170–1189, 2017.
13. Wong, K. T., Y. Song, C. J. Fulton, S. Khan, and W.-Y. Tam, "Electrically long dipoles in a collocated/orthogonal triad — For direction finding and polarization estimation," *IEEE Transactions on Antennas and Propagation*, Vol. 65, 6057–6067, 2017.

14. Kitavi, D. M., K. T. Wong, M. Zou, and K. Agrawal, "A lower bound of the estimation error of an emitter's direction-of-arrival/polarization, for a collocated triad of orthogonal dipoles/loops that fail randomly," *IET Microwaves, Antennas and Propagation*, Vol. 11, 961–970, 2017.
15. Au-Yeung, C. K. and K. T. Wong, "CRB: Sinusoid-sources estimation using collocated dipoles/loops," *IEEE Transactions on Aerospace and Electronic Systems*, Vol. 45, 94–109, 2009.
16. Xu, Y., Z. Liu, K. T. Wong, and J. Cao, "Virtual-manifold ambiguity in HOS-based direction-finding with electromagnetic vector-sensors," *IEEE Transactions on Aerospace and Electronic Systems*, Vol. 44, 1291–1308, 2008.
17. Wong, K. T., "Direction finding/polarization estimation — Dipole and/or loop triad(s)," *IEEE Transactions on Aerospace and Electronic Systems*, Vol. 37, 679–684, 2001.
18. Wong, K. T., "Blind beamforming/geolocation for wideband-FFHs with unknown hop-sequences," *IEEE Transactions on Aerospace and Electronic Systems*, Vol. 37, 65–76, 2001.
19. Wong, K. T. and M. D. Zoltowski, "Uni-vector-sensor ESPRIT for multisource azimuth, elevation, and polarization estimation," *IEEE Transactions on Antennas and Propagation*, Vol. 45, 1467–1474, 1997.
20. Cheng, Q. and Y. Hua, "Performance analysis of the MUSIC and Pencil-MUSIC algorithms for diversely polarized array," *IEEE Transactions on Signal Processing*, Vol. 32, 284–299, 1996.
21. Wong, K. T. and M. D. Zoltowski, "Self-initiating MUSIC direction finding and polarization estimation in spatio-polarizational beamspace," *IEEE Transactions on Antennas and Propagation*, Vol. 48, 1235–1245, 2000.
22. Zoltowski, M. D. and K. T. Wong, "ESPRIT-based 2D direction finding with a sparse array of electromagnetic vector-sensors," *IEEE Transactions on Signal Processing*, Vol. 48, 2195–2204, 2000.
23. Li, J. and R. T. Compton, "Angle and polarization esrimation using ESPRIT with a polarization sensitive array," *IEEE Transactions on Antennas and Propagation*, Vol. 39, 1376–1383, 1991.
24. Miron, S., Y. Song, D. Brie, and K. T. Wong, "Multilinear approach of direction finding using a sensor-array with multiple scales of spatial invariance," *IEEE Transactions on Aerospace and Electronic Systems*, Vol. 51, 2057–2070, 2015.
25. Wong, K. T. and M. D. Zoltowski, "Direction-finding with sparse rectangular dual-size spatial invariance arrays," *IEEE Transactions on Aerospace and Electronic Systems*, Vol. 34, 1320–1336, 1998.
26. Wong, K. T. and M. D. Zoltowski, "Closed-form direction-finding with arbitrarily spaced electromagnetic vector-sensors at unknown locations," *IEEE Transactions on Antennas and Propagation*, Vol. 48, 671–681, 2000.
27. Zoltowski, M. D. and K. T. Wong, "Closed-form eigenstructure-based direction finding using arbitrary but identical subarrays on a sparse uniform rectangular array grid," *IEEE Transactions on Signal Processing*, Vol. 48, 2205–2210, 2000.
28. Pal, P. and P. P. Vaidyanathan, "Nested arrays: A novel approach to array processing with enhanced degrees of freedom," *IEEE Transactions on Signal Processing*, Vol. 58, 4167–4181, 2010.
29. Vaidyanathan, P. P. and P. Pal, "Sparse sensing with co-prime samplers and arrays," *IEEE Transactions on Signal Processing*, Vol. 59, 573–586, 2011.
30. Zhou, C., Z. Shi, and Y. Gu, "DECOM: DOA estimation with combined MUSIC for coprime array," *IEEE Int. Conf. Wireless Commun. Signal Process. (WCSP)*, 1–5, 2013.
31. Liu, C. L. and P. P. Vaidyanathan, "Remarks on the spatial smoothing step in coarray MUSIC," *IEEE Signal Process. Lett.*, Vol. 22, 1438–1442, 2015.
32. Boudaher, E., Y. Jia, F. Ahmad, and M. G. Amin, "Multi-frequency co-prime arrays for high-resolution direction-of-arrival estimation," *IEEE Signal Process.*, Vol. 63, 3797–3808, 2015.
33. Pal, P., P. P. Vaidyanathan, F. Ahmad, and M. G. Amin, "Coprime sampling and the MUSIC algorithm," *IEEE Digital Signal Proc. Workshop and IEEE Signal Proc.*, Vol. 47, 289–294, 2011.
34. Friedlander, B. and A. J. Weiss, "Direction finding using spatial smoothing with interpolated arrays," *IEEE Transactions on Aerospace and Electronic Systems*, Vol. 28, 574–587, 1992.

35. Shi, Z., C. Zhou, Y. Gu, and N. A. Goodman, "Source estimation using coprime array: A sparse reconstruction perspective," *IEEE Sensors Journal*, Vol. 17, 755–765, 2017.
36. Tan, Z., Y. C. Eldar, and A. Nehorai, "Direction of arrival estimation using co-prime arrays: A super resolution viewpoint," *IEEE Transactions on Signal Processing*, Vol. 62, 5565–5576, 2014.
37. Qin, S., Y. D. Zhang, and M. G. Amin, "Generalized coprime array configurations for direction-of-arrival estimation," *IEEE Transactions on Signal Processing*, Vol. 63, 1377–1390, 2015.
38. Dong, W., M. Diao, L. Gao, and L. Liu, "A low-complexity DOA and polarization method of polarization-sensitive array," *Sensors*, Vol. 17, 2017.
39. Zhang, Y. D., M. G. Amin, and HB. imed, "Sparsity-based DOA estimation using co-prime arrays," *Proc. IEEE Int. Conf. Acoust., Speech, Signal Process. (ICASSP)*, 3967–3971, 2013.